

NO-A082 530 NAVAL ACADEMY ANNAPOLIS MD DIV OF ENGINEERING AND WEAPONS F/6 20/4
SOME EXPERIMENTAL RESULTS WITH SHIP MODEL ACCELERATION WAVES, (U)

UNCLASSIFIED

NL

 $\Delta T_{\text{eff}} = 30^\circ\text{C}$

GATE

FALME 50

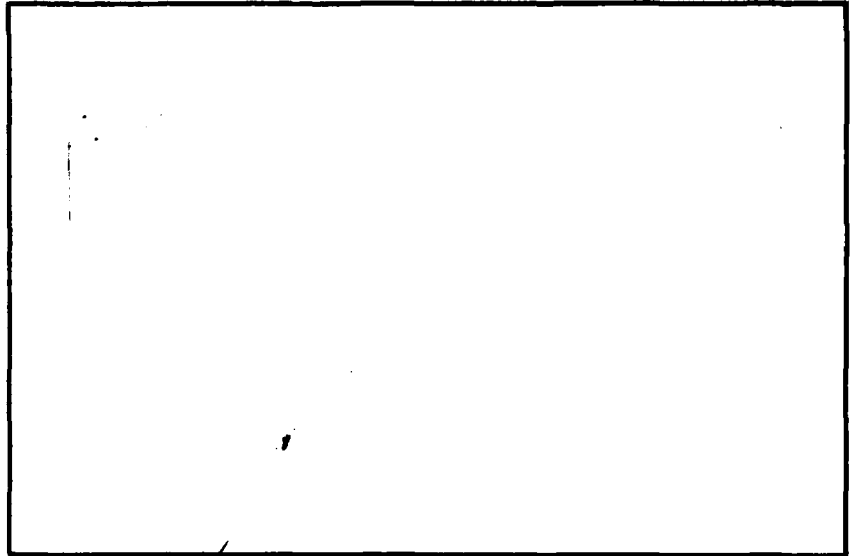
5-8

DTIC

DTIC
ELECTE
APR 1 1980

20
SC

AD A 082530



LEVEL

This document has been approved
for public release and sale; its
distribution is unlimited.

UNITED STATES NAVAL ACADEMY
DIVISION OF
ENGINEERING AND WEAPONS
ANNAPOLIS, MARYLAND

DDC FILE COPY

DEPARTMENT OF THE NAVY
United States Naval Academy
Annapolis, Maryland 21402

Division of Engineering and Weapons

20
(14) USNA-
Report No EW-4-80

(6) SOME EXPERIMENTAL RESULTS WITH
SHIP MODEL ACCELERATION WAVES,

(10) S. M. Calisal*

(11) February 1980

(12) 44

DTIC
ELECTE
APR 1 1980
S D
C

Approved for public release
Distribution Unlimited

*Assistant Professor
Naval Systems Engineering Department
U. S. Naval Academy
Annapolis, Maryland

406923

dm

NOMENCLATURE

C Ship speed

L Ship length

g Gravitational acceleration

$k_o \frac{g}{CL}$

t Time

T A large time

f_e Encounter frequency $f_e = \frac{g}{8\pi c}$

ϕ A velocity potential

m Source strength

f Location of the source

Fr Froude number

Accession For	
NTIS GRA&I	<input checked="" type="checkbox"/>
DOC TAB	<input type="checkbox"/>
Unannounced Justification	
By	
Distribution/	
Availability Codes	
Dist	Avail and/or special
A	

TABLE OF CONTENTS

Nomenclature	1
Abstract	1
Introduction	1
Time dependent wave system	3
Experiments	4
Results of Experiments	5
Discussion of Results and Conclusions	10
Bibliography	13
Acknowledgement	14
Appendix A	15
Tables and Figures	17

ABSTRACT

The wave resistance of a ship moving at a constant speed can be calculated using information obtained from its wave pattern. One of the basic assumptions in wave survey methods is the existence of a time-independent model speed.

In towing tanks initial acceleration is unavoidable. Wehausen (1964) showed that the effect of initial acceleration on wave resistance has a decaying and oscillating character. Calisal (1977) gave the general form of the initial acceleration potential and showed the existence of a two-dimensional wave of the form:

$$\zeta_T = \frac{A}{cT} \sin \left(\frac{1}{2} k_0 (x - cT) + \phi(t) \right) + O(cT)^{-2}.$$

To study the validity of the theoretical results some experiments were performed. The variation of the measured spectra and the frequencies within the recorded total resistance pitching moment are of interest. Results indicate that models should travel a distance proportional to the square of the Froude number before wave data collection can be begun, that the predicted encounter frequency exists in the recorded total resistance and pitching moment signals, and that special effort is required to avoid initial acceleration waves due to wall effects.

INTRODUCTION

Wave resistance of ships can be calculated by using some data related to their wave pattern [1], [2], [3].* Different methods are based on the existence of a potential flow that describes the ship wave system. The wave resistance problem is usually studied in a linearized form, and one assumes a constant ship or model speed. In towing tanks, however, initial acceleration

*Numbers in brackets designate References at end of paper

is unavoidable. It is therefore necessary to estimate the effect of initial acceleration on the measured wave resistance values.

In engineering analysis the transient effects are usually not studied when the steady solution is observed to be stable, either experimentally or "intuitively". Transient effect or their possible interaction with the steady state solution are neglected, and the mean measured quantities are assumed to represent the steady solution. Wehausen [4] in his Weinblum memorial lecture explained how such effects can be unexpectedly misleading or important. The waves generated by a model accelerating to reach a uniform speed fall in the same category, although some analytic and numerical work does exist on the subject.

The effect of initial acceleration upon the wave resistance of a ship was studied by Wehausen [5]. This work shows that the wave resistance calculated for a ship model, instantaneously brought to a constant speed, will have an oscillating and decaying behavior, and that the "mean" value of the oscillation will correspond to Michell's wave resistance. Calisal [6] studied the effect of initial acceleration on ship wave pattern and wave survey methods. That study shows that Wehausen's [5] solution is in fact the resistance of a ship moving in a decaying two dimensional wave system given by:

$$\zeta = \frac{A}{cT} \sin \left(\frac{1}{4} k_0 (x - cT) + \phi(t) \right) + O(cT)^{-2}, \quad (1)$$

indicating that the initial acceleration waves about the ship will have a sinusoidal shape, their length will be four times larger than the steady transverse waves, and their amplitude will decay with time. These transient waves will also move with a speed c with respect to the ship. This almost monochromatic wave gives indications that it can easily be detected and filtered out using numerical calculations.

If the mathematical procedure employed in the above analysis is correct, then one would expect to have an encounter frequency resulting from the relative motion of the ship and the initial acceleration waves. The encounter frequency given by this analysis is $f_e = \frac{g}{8\pi c}$. If again the mathematical formulation of the problem corresponds to the physical phenomenon, then the steady state wave pattern should develop a sufficient time after the start, and the only time dependence should be associated with the wave system given by equation 1. In order to test the theory a series of experiments was designed to find:

- a. time dependence of the observed spectra after the initial acceleration,
- b. the existence of the initial acceleration wave given by equation (1),
- c. the existence of an encounter frequency predicted by the theory.

TIME DEPENDENT WAVE SYSTEM

The asymptotic velocity potential associated with an impulsive start of a source in a frame moving with the source (see Figure 1) is given by Calisal as:

$$\phi_{2T} = \frac{4\sqrt{2m}}{(cT)} \exp\left(\frac{k_0}{4}(z-f)\right) \cos\left[\frac{k_0}{4}(x-cT)\right] + O(cT)^{-2} \quad (2)$$

ϕ_{2T} corresponds to a wave system superimposed on the steady wave pattern of the source. Since the total wave height is recorded, a time dependent error will be introduced. The contribution of ϕ_{2T} to the wave generated by a source is:

$$\zeta_T = \frac{1}{g} (\phi_{2T,t} - c\phi_{2T,x}) \quad z = 0,$$

or

$$\zeta_T = \frac{A}{cT} \sin\left(\frac{1}{4} k_0 (cT - x)\right) + O(cT)^{-2}$$

where

$$A = \frac{2\sqrt{2m}}{c} \exp\left(-\frac{k_0 f}{4}\right). \quad (3)$$

We can therefore conclude that the amplitude of the time-dependent wave will decrease linearly with time, and that the wave number will be constant and equal to $\frac{k_0}{4}$. As the time dependent waves are moving with respect to the source or to the ship, the ship is in fact sailing not on a smooth surface but on her own acceleration waves. This would generate an unsteady wave resistance. The decaying amplitude will ensure that the effect of ζ_T will be zero as $T \rightarrow \infty$. One can also show that any other type of acceleration will only change the phase of the initial acceleration wave and that equation (1) is therefore the most general form of the initial acceleration wave to the order $(\frac{1}{cT})$.

EXPERIMENTS

The experiments reported here were carried out in the 120 ft tank of the Hydrodynamic laboratory at the U.S. Naval Academy. Three different sets of experiments were performed. During the first set of experiments the quantities of interest were the apparent wave lengths in the recorded wave height record and the dependence of the wave spectrum on the distance travelled by the model. The model used was a five foot long series 60 block 60 model. To avoid model motion-induced waves, the model was rigidly fixed to the carriage. Two sonic wave height gages were located 17 and 24 inches off the tow line. The model was accelerated to the desired speed at the highest available rate and the distance from the bow of the model to the wave height gages was changed from 1 to 4 model lengths. Five different model speeds were selected. The Model Froude number (Fr) remained in the range $.2 < Fr < .4$. The wave height records along the length of the model were recorded to calculate wave resistance values by a well-known procedure based on longitudinal-cut wave survey methods [2].

During the second set of experiments the quantities of interest were the frequencies in the total resistance signal and the pitching moment signal of the model following initial acceleration. The model was first attached free to surge, heave and pitch. The high initial acceleration resulted in a high pitch angle disturbing the free wave system and possibly the assumptions in the theory. This forced the removal of the degree of freedom for pitching and the model remained free to heave and surge only during these experiments. The total resistance and pitching moment signals are recorded for frequency analysis. The model speeds for the second set of experiments were the same as for the first set.

In the third set of experiments that followed the purpose was to isolate the ship acceleration wave. Appendix A shows that the asymptotic expression for the velocity potential resulting from a suddenly stopped model is equal to the velocity potential corresponding to a suddenly accelerated one with a minus sign. This study gave the possibility of visual observation and isolation of initial acceleration waves. Pictures of the wave profiles were taken, and wave height data were recorded by three gages located on a line parallel and perpendicular to the tank wall. The purpose in the selection of the wave height probe location was to check the two dimensionality of the initial acceleration waves and to record the changes in the wave spectra as observed by probes located at a different distance from the initial acceleration location. The rigidly fixed model was stopped 10 feet away from the first probe. The probes were separated by a distance of 5 feet and fixed in the tank frame. The electronic signals were conditioned by a low pass 10 Hz filter.

RESULTS OF THE EXPERIMENTS

The data processing and results corresponding to each set of experiments will be presented separately, beginning with the first, which can be summarized

as follows. A typical longitudinal-cut wave height is given in Figure 2. The reflection of the bow wave from the tank wall is easily distinguishable. From the recorded wave height data the Fourier transform of the longitudinal cut is obtained as:

$$C(s, \bar{y}) + i S(x, \bar{y}) = \int_{-\infty}^{+\infty} \bar{\zeta}(\bar{x}, \bar{y}) \exp(is\bar{x}) d\bar{x} \quad (4)$$

The value $(C^2 + S^2)^{1/2}$ is usually called the amplitude spectrum. The wave pattern is assumed to be transversely symmetric and the wave resistance is calculated as:

$$\bar{R}_w = \frac{1}{\pi} \int_0^{\infty} \frac{s^2 - 1}{s^2 (2s^2 - 1)} (C^2 + S^2) du, \quad (5)$$

where $s = \sec\theta$, $u = \sec\theta \tan\theta$, in the direction of the propagation of the free waves. s and u are longitudinal and transverse wave numbers, and are kinematically connected. Barred (-) variables represent dimensionless variables. The fundamental units taken are ship speed c , density of the fluid ρ , and gravitational acceleration g . $k_0 = -g/c^2$, which has the dimension (L^{-1}) , is used to nondimensionalize lengths. The resistance is nondimensionalized as $R = R_w k_0^2 / \rho c^2$. The computer program used for the computation of the resistance has been reported by Reed [7]. Results of the calculated resistance coefficients are given in Table 1. Channel one refers to the sonic probe located 24 inches off the tow line and channel two to the sonic probe located 17 inches off the same line. The growth of the amplitude spectrum with time, and its dependence on the transverse location of the probe are of interest. In all cases studied the spectrum changed as the distance from the start line to the probe line was changed. An example of this can be seen in Figure 3. The spectra and their corresponding wave resistance values are seen to increase as the distance travelled at the constant speed, c , increases. Resistance values on the diagram are equal to $114 \times R_w$ given in equation (5). Figures 4, 5, and 6 show the differences in spectra as seen by two wave height probes.

The variable L represents the distance between the probe and the model before acceleration. One can observe from the vertical scales that the spectra grow with the distance traveled, and that as the traveled distance increases, so do the spectral similarities. One can also see that when a short distance is traveled before data collection, the outer probe records a smaller energy level or resistance than the inner probe closer to the tow line.

At low speeds, such as Froude number 0.245, the "convergence" of the spectra is shown in Figure 7. At a medium speed corresponding to Froude number 0.272 the convergence seems to require that more distance be traveled, as shown in Figure 8.

In Figure 7 and 8 one can see a small hump in the spectra corresponding to $s = .5$. This is the point about which the initial acceleration wave given by equation (1) should in fact be observed. The wavelength of the initial acceleration waves is four times the wavelength of the ship's transverse waves and it is numerically very difficult to determine the existence of this wave from relatively short records. Short records are imposed as only a portion of the recorded longitudinal wave height record can be used because of the reflections from the tank walls. A larger towing tank will permit the usage of longer records and the more accurate frequency analyses of longer waves.

Nondimensional wave resistance values obtained by dividing the wave resistance computed from the wave profiles recorded in these experiments by the wave resistance values experimentally reported by Ward [3] for the same model are plotted versus the variable $k_0 c T / 4$ (Figure 9). This plot suggests that to reach the steady state, $k_0 c T / 4$ should be larger than 10, or the distance traveled at constant speed c should be larger than $40 c^2 / g$. For a 5' ship model moving at Froude number .3 the corresponding distance is 18', but for the same model moving at Froude number .4 this distance is 32'. The above

requirement for distance traveled longer than $40 c^2/g$ is equivalent to $n < 40 F^2$ where n is distance traveled divided by ship length. The above formula, therefore, brings the Froude number in the computation to the required minimum distance traveled before data collection. This might also be used to calculate the maximum permissible Froude number one can experiment at in a given tank for wave survey analysis. Before analyzing the results of the second set of experiments were analyzed the numerical example by Wehausen [4] was studied and a very good correspondence between the expected frequency and the frequency of oscillations in the above-mentioned example was observed. Even though wave resistance is only a portion of the total resistance, it was decided to study the total resistance signal for the existence of an initial acceleration-induced encounter frequency. A typical plot of the measured total resistance is given in Figure 10. The portion of the signal oscillating about a mean value was selected and the related spectrum was calculated by a Fourier transform method. Figures 11, 12 and 13 show the spectra of the oscillations superimposed on the mean value of the model total resistance. The vertical line indicates the encounter frequency predicted by potential flow solutions. In all 12 runs corresponding to 6 different speeds a local peak was found very close to the predicted encounter frequency. It is not clear yet what the sources of the other peaks are. Some of them are actually larger than the peak which one can identify as the encounter frequency.

The initial acceleration wave is expected to generate a pitching moment at the encounter frequency f_e . The frequency spectrum of this pitching moment was also studied. This analysis showed that a pitching moment does in fact exist at the predicted frequency and that no other frequencies are observed to be in the same range, in contrast to what was observed for the total resistance records. Figure 14 shows the portion of the spectrum below the resonance frequency of the system which was measured to be 2 Hertz. The plot of the

observed peak frequency versus the ship mean velocity (Figure 15) shows that frequencies given by pitching moment data follow the theoretical curve more closely than the data corresponding to the total resistance, and that the agreement is better at lower speeds.

The last series of experiments concentrates on the form of the acceleration waves generated by a suddenly stopped model. The visual observations can be summarized as follows. As the ship stops a complex wave is generated about the hull. Shortly there after, an almost two-dimensional wave is seen to propagate along the length of the tank. After a finite amount of time the tank surface is observed to be covered by a complex wave system. The picture (Figure 16) shows the almost two-dimensional wave observed. Figure 17 shows the wave height records observed by three wave height gages located on a line perpendicular to the tow line. An almost two-dimensional wave pattern can be observed Figure 18, which shows the expected decaying waves followed by waves of higher frequency and amplitudes. The existence of this type of complex waves is explained by Wehausen [4], as image sources due to the tank walls.

The frequency spectra of the signals obtained from some probes aligned parallel to the tow line were also obtained. Two signal durations were used for these calculations. One duration is comparable to the time span required by wave survey methods and the other is 30 seconds, which is the total data collection time per run. The first duration is of the order of 3 to 4 seconds and corresponds to the time span between the time the bow of the ship is aligned with the probe and the first reflected wave is recorded by the probe. This portion of the data is labelled short data, and the complete record length long data. The high peaks which were observed in the frequency spectra that were analyzed and the expected theoretical frequencies are listed in Table 2. One can observe that the short data that correspond to data collection for

wave survey analysis have a high peak at a frequency outside of the frequency spectrum of interest. The long data, on the other hand give a large peak in the portion of the spectrum to be used with wave survey methods. Figures 19 and 20 show a pair of spectra corresponding to the short and long data respectively. There seems to exist the possibility that wave survey data can be collected in such a way as to eliminate or filter out the initial acceleration waves. This operation will be easier in relatively wide tanks, since the disturbances generated by image sources will be less important. The other solution for eliminating initial acceleration waves is to wait a long enough time, so as to reduce the significance of the accelerating waves.

DISCUSSION OF THE RESULTS AND CONCLUSION

To study the applicability of potential flow solutions to transient ship problems and to check the correspondence between experimental and theoretical quantities, a series of experiments were performed. Intuitively, one would expect that a certain amount of time would have to pass for a system to reach a steady state. Steady state for a ship wave system means that the waves will extend far away from the ship back to infinity. Potential theory predicts that if the parameter $\frac{koct}{4}$ is large, the potential flow around the ship will be the sum of a term corresponding to the steady state and time-dependent term decaying as $\frac{1}{ct}$. More commonly, if the distance traveled by the model is large, one expects to duplicate the steady state flow. The experiments show that the recorded ship spectrum changes with time as the model moves at a constant speed after initial acceleration. This effect is stronger at higher Froude numbers. The largest changes in spectra occur at about the ship transverse wavelength or $s = 1$. This might explain some discrepancies or scatter of wave resistance values computed by wave survey methods.

One can also observe that it requires more time for the spectrum to develop at channel 1 further away from the tow line. As the wave height probes were relatively close to each other, a final result cannot be obtained, but the data suggest that it will take a longer time for the spectrum to develop at a larger distance from the tow line. This resembles the concept of "fetch" used in oceanographic studies. To transfer a certain amount of energy to the surrounding system the ship model has to move a certain distance and it will require additional time for this energy to propagate in the transverse direction.

Experiments show that the number of model lengths "n" a ship has to move at constant speed for a successful wave survey analysis can be obtained by the equation

$$n \geq 40 F^2$$

Experiments also indicate that the total resistance signal contains frequencies other than the expected encounter frequency, whereas, the pitching moment signal shows mainly an encounter frequency. This evidence suggests that viscous effects might be responsible for the additional frequencies. It was also observed that, as the Froude number increased the measured encounter frequencies decreased faster than predicted by the theory. One can conjecture that at higher Froude numbers assumptions used for linearizations are less valid than at lower Froude numbers.

The deceleration waves showed that an almost two-dimensional long wavelength wave exists for a finite time at the wave probe, and that three-dimensional, higher frequency waves follow the first train of waves. As there is a time delay between low frequency and high frequency waves, and usually only a finite wave record is used for wave survey methods obtained during a relatively short time, high frequency waves related to the image sources can possibly be avoided and the asymptotic, long wavelength can be filtered out of

the record. It is expected that wider towing tanks will have less error due to initial acceleration waves.

Bibliography

1. Eggers, K., "Über die Ermittlung des Wellenwiderstandes eines Schiffsmodells durch Analyse seines Wellensystems, I, II, "Schiffstechnik, vol. 9, (1962), pp. 79-85 vol. 10 (1963), pp. 93-106.
2. Sharma, S. D. (1966), "An Attempted Application of Wave Analysis Technique to achieve Bow-Wave Reduction," Sixth Symposium on Naval Hydrodynamics, Washington, D.C., U. S. Printing Office, pp. 231-273.
3. Ward, L. W., "Experimental Determination of Ship Wave Resistance from the Wave Pattern," Webb Institute of Naval Architecture 1963, Glen Cove, N.Y., viii + 68 pp.
4. Wehausen, J. V., 1979; "Ship Theory, Ship Design and George Weinblum", Institut für Schiffbau der Universität Hamburg Report 376, July 1979.
5. Wehausen, J. V., "Effects of Initial Acceleration Upon the Wave Resistance of Ship Models," J. Ship Research vol. 7, no. 3, pp. 38-50 (1964).
6. Calisal, S. M., "Effect of Initial Acceleration of Ship Wave Pattern and Wave Survey Methods," J. Ship Research, vol. 21, no. 4, Dec 1977, pp. 239-247.
7. Reed, A. M., Documentation for a series of computer programs for analyzing longitudinal wave cuts and designing bow bulks, DTNSRDC/SPD-0820-01, June 1979.

Acknowledgement

The author would like to express his appreciation to Ronald Altmann and John Hoyt for their continuous help during the experiments and the computerized data collection phase. Special thanks are also extended to Sharon Vaughn for typing this manuscript.

APPENDIX A

POTENTIAL FOR A SUDDENLY STOPPED SOURCE

In a frame of reference fixed on the source moving in a + x direction the portion of the velocity potential responsible for surface waves can be written as:

$$\phi_w(x, y, z, t) = \frac{\sqrt{g}}{\pi} \int_{-T^*}^t m(\tau) d\tau \int_{-\pi}^{\pi} d\theta \int_0^{\infty} \sin[\sqrt{kg}(t-\tau)] \exp(k[(z-f)+i\bar{\omega}]) \sqrt{k} dk \quad (1)$$

$\bar{\omega} = (x + \int_{\tau}^t c(\tau) d\tau) \cos\theta + y \sin\theta$, the coordinate of the source is $(0,0,-f)$ and m is the source strength. The following asymptotic expansion for large time $t \gg 1$ can be obtained for a source moving at constant speed c within the time interval $T^* < t < 0$ and speed equal to zero for $t > 0$. T^* is assumed to be a large time to be replaced by $-\infty$ after the integration. The integration of the time dependent terms of (1) result in two parts.

$$\begin{aligned} \int_{T^*}^t \sin(\sqrt{kg}(t-\tau)) \exp(i k [(t-\tau) c \cos\theta]) d\tau = \\ \frac{e^{iKc \cos(t+T^*)}}{k g - k^2 c^2 \cos^2\theta} [i k c \cos\theta \sin(\sqrt{kg}(t+T^*)) - \sqrt{kg} \cos(kg(t+T^*))] \\ - \frac{e^{-k c \cos t}}{kg - k^2 c^2 \cos^2\theta} [i k c \cos\theta \sin(\sqrt{kg} t) - \sqrt{kg} \cos(\sqrt{kg} t)] \end{aligned}$$

The first can be thought of as the sum of all impulses from T^* to 0 and the second term the contribution of the jump at $\tau = 0$.

One can show that the contribution of the first term in fact is equal to zero for $T^* \rightarrow -\infty$. The remaining integral therefore for ϕ_w is:

$$\phi_w(x, y, z, t) = \frac{\sqrt{g} m}{\pi c^2} \int_{-\pi}^{\pi} d\theta \int_0^{\infty} dk \exp(k(z-f)) k^{\frac{1}{2}} \exp(i(k x \cos\theta + ky \sin\theta))$$

$$\left[\frac{i k c T \cos \theta (i k c \cos \theta \sin \sqrt{k g} T - \sqrt{k g} \cos(\sqrt{k g} T))}{-k^2 c^2 \cos^2 \theta + k g} \right]$$

This is again negative of the term that one finds for the velocity potential of a source for an impulsive start studied in Calisal [6]. That study gives the asymptotic form of the equation above. The meaning of large T in the equation above on the other hand is the time elapsed from the moment the model stops.

WAVE RESISTANCE COEFFICIENTS

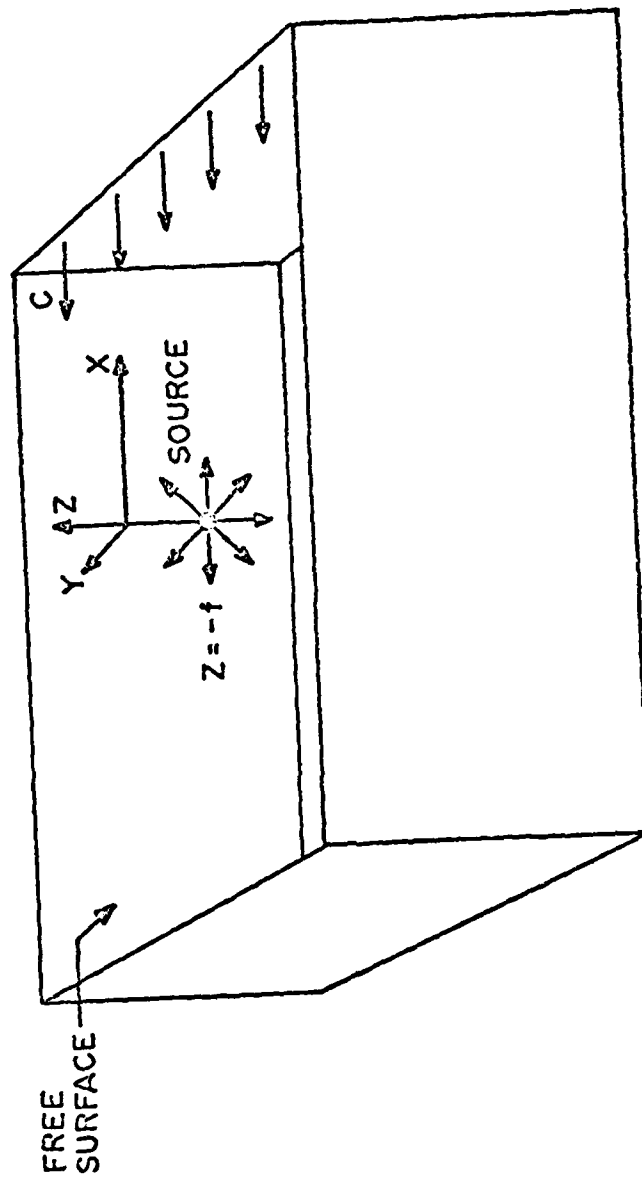
RUN NUMBER	VELOCITY IN KNOTS	CR CHANNEL 1	CR CHANNEL 2	DISTANCE TRAVELED
1	1.835	1.19798E-4	1.24777E-4	1L
2	1.635	1.23999E-4	1.34443E-4	2L
3	1.839	1.29823E-4	1.3945E-4	3L
4	1.676	1.19799E-4	1.24777E-4	1L
5	2.039	1.23999E-4	1.34443E-4	2L
6	2.042	1.29823E-4	1.3945E-4	3L
7	2.354	2.11669E-4	2.52699E-4	1L
8	2.355	3.11677E-4	4.69127E-4	2L
9	2.37	4.49162E-4	4.69234E-4	3L
10	2.576	7.01923E-4	1.12672E-3	1L
11	2.58	1.31823E-3	1.3945E-4	2L
12	2.554	1.47356E-3	1.33749E-3	3L
13	2.892	1.03857E-3	1.34115E-3	1L
14	2.927	1.36667E-3	1.39444E-3	2L
15	2.832	1.30861E-3	1.27833E-3	3L

TABLE 1

FREQUENCY CORRESPONDING TO MAXIMUM AMPLITUDE IN WAVE SPECTRUM

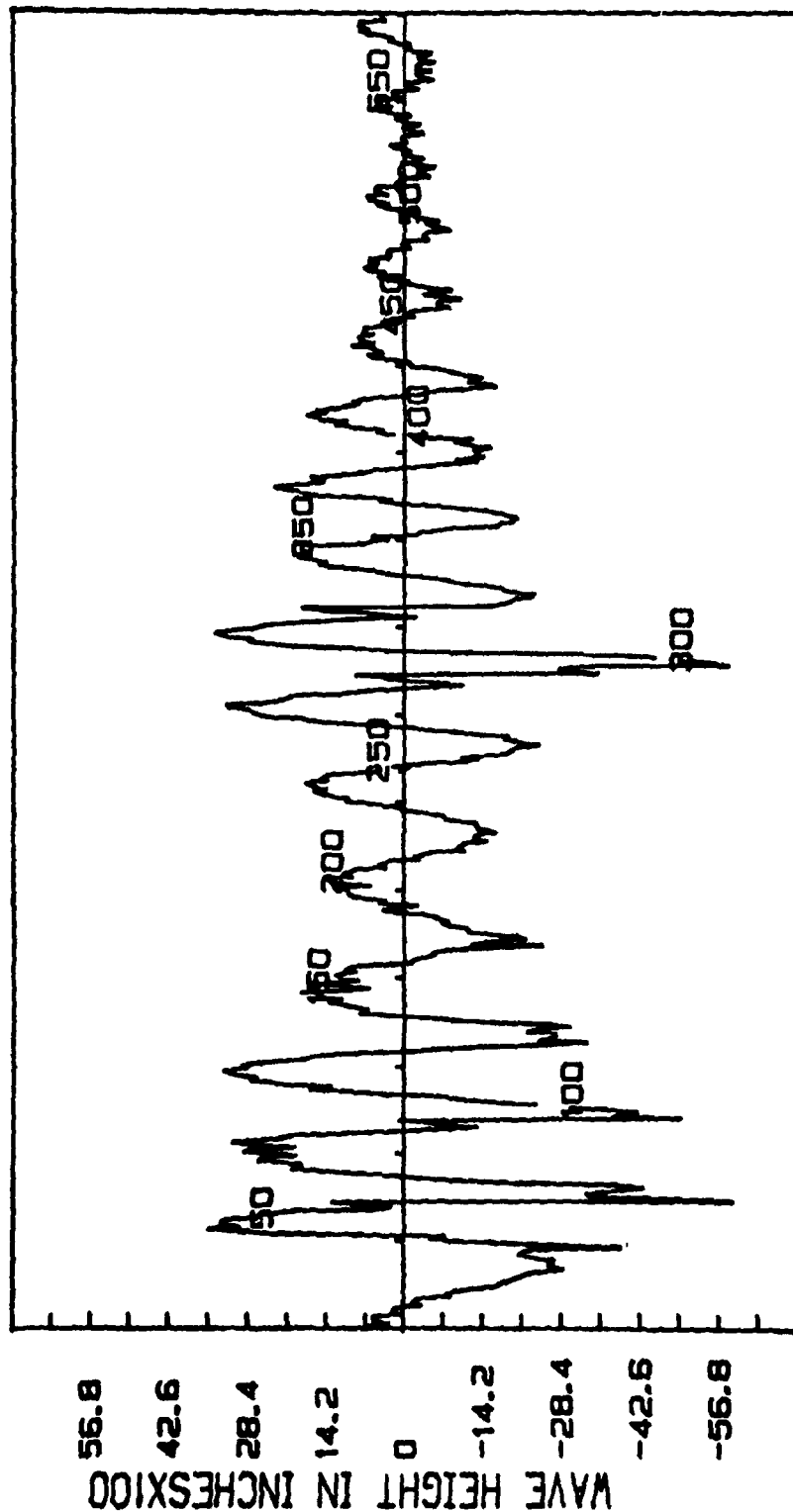
RUN	SPEED FT/SEC	FREQUENCY FOR S = 1	RECORD 1	RECORD 2	RECORD 3
1 Short Data	3.2	1.57	1	.8	.8
1 All Data	3.2	1.57	2.5	1.9	1.6
3 Short Data	3.6	1.4	.75	1.3	.9
3 All Data	3.6	1.4	1.5	1.5	1.5
5 Short Data	3.95	1.28	.75	1.1	.9
5 All Data	3.95	1.28	1.41	1.5	1.55
7 Short Data	4.31	1.18	1.1	1.1	.9
7 All Data	4.31	1.18	1.2	1.8	1.1
11 Short Data	5.1	.99	.5	1.1	.8

Table 2



COORDINATE SYSTEM AND THE LOCATION OF THE SOURCE
FIGURE 1.

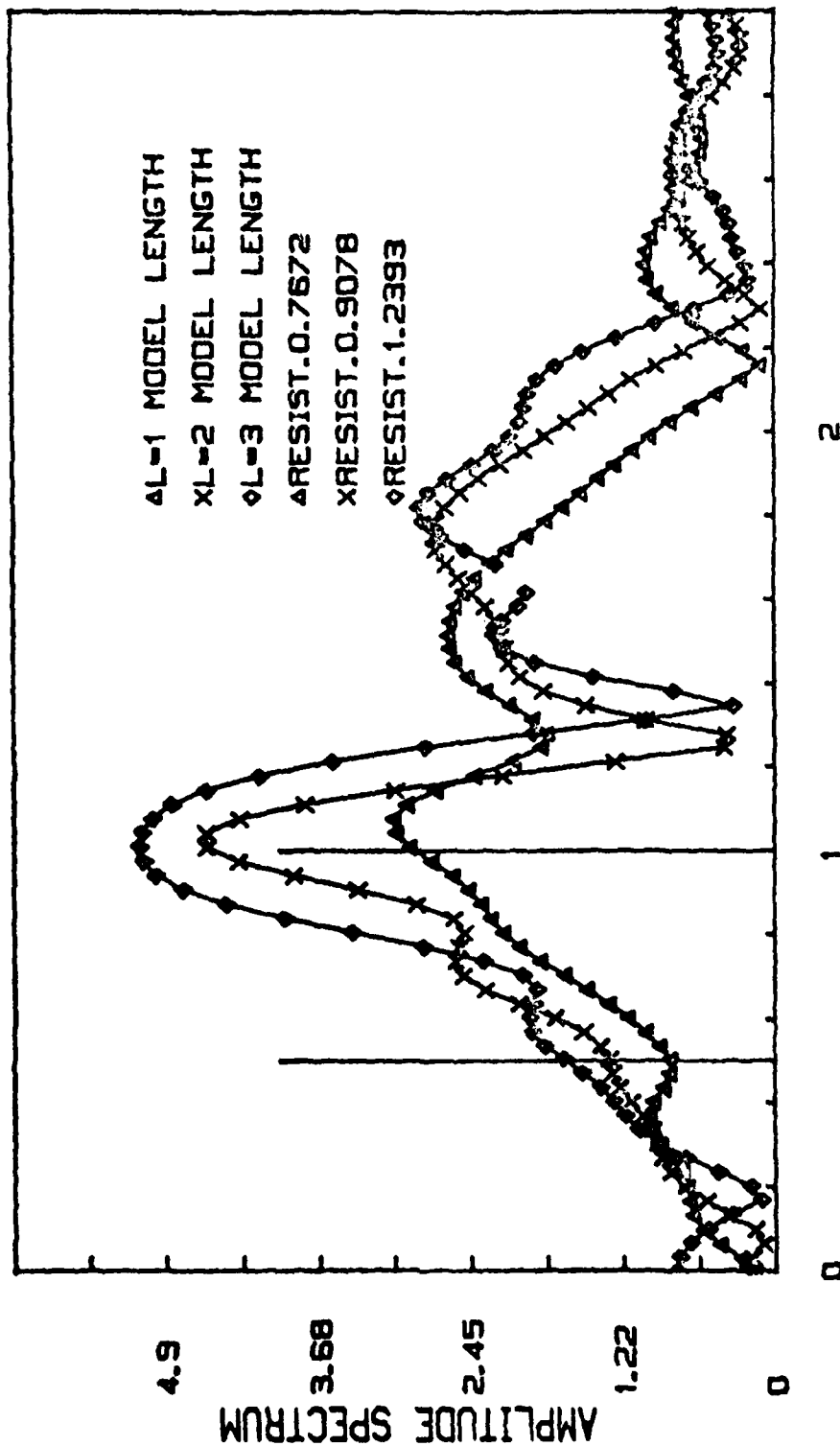
WAVE HEIGHT AT FROUDE NR 0.315



TIME DATA SERIES 60 CB 60 RUN 9

Figure 2

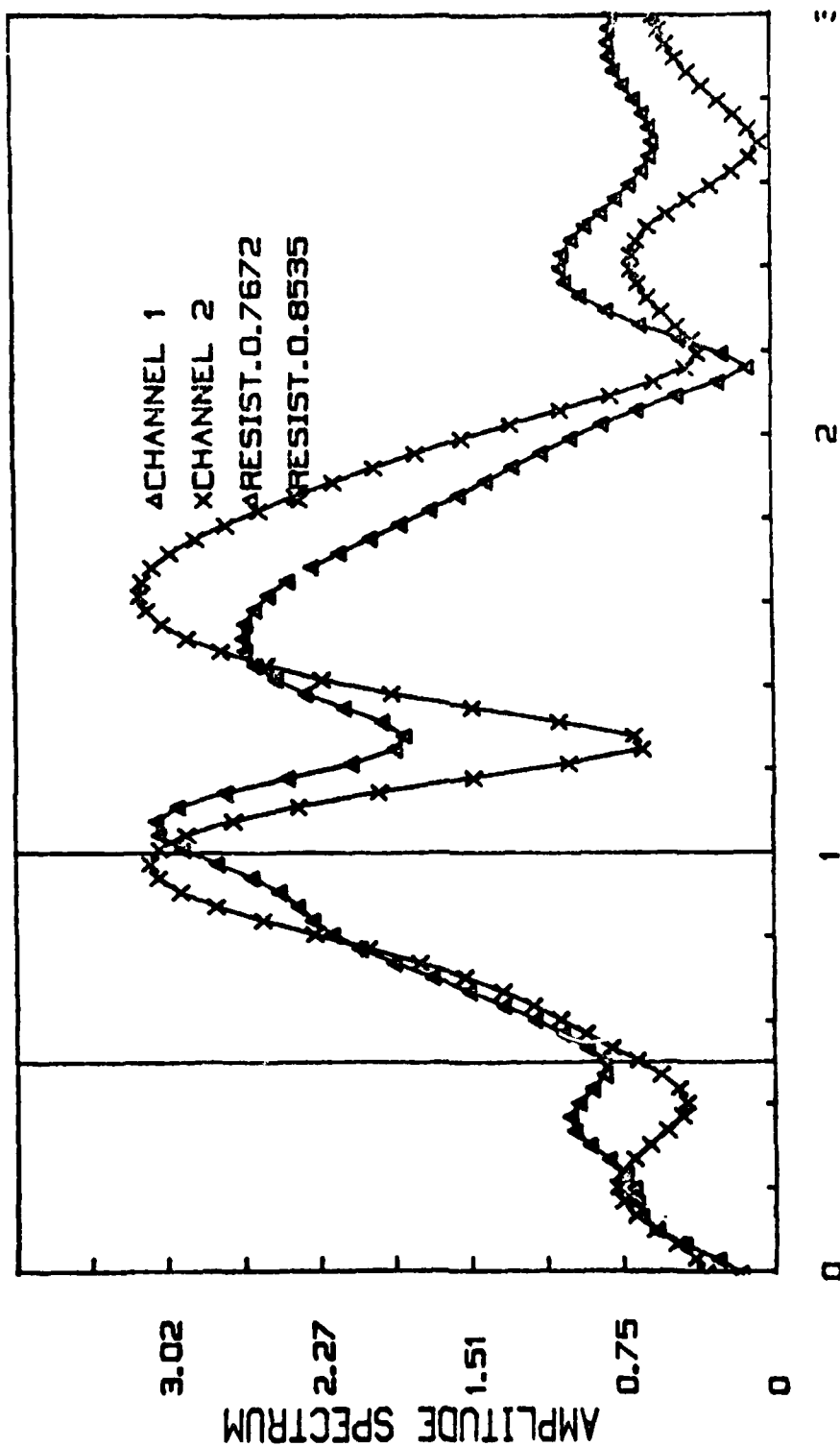
SPECTRUM AT FROUDE NR=0.377



S VALUE SERIES 60 CB60 RUN 13

Figure 3

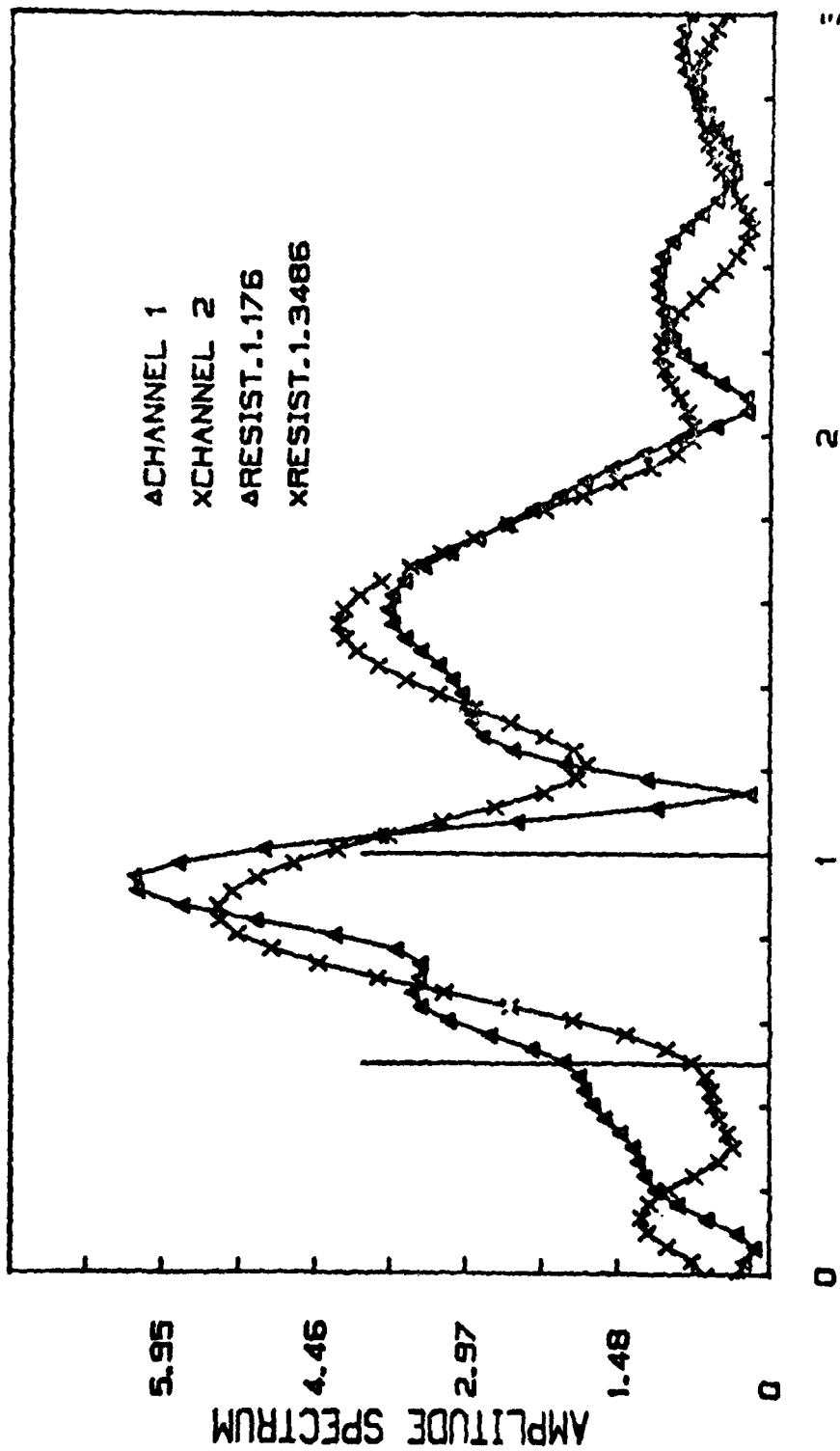
SPECTRUM AT FROUDE NR=0.374



S VALUE SERIES 60 CB60 RUN 13 L = 5'

Figure 4

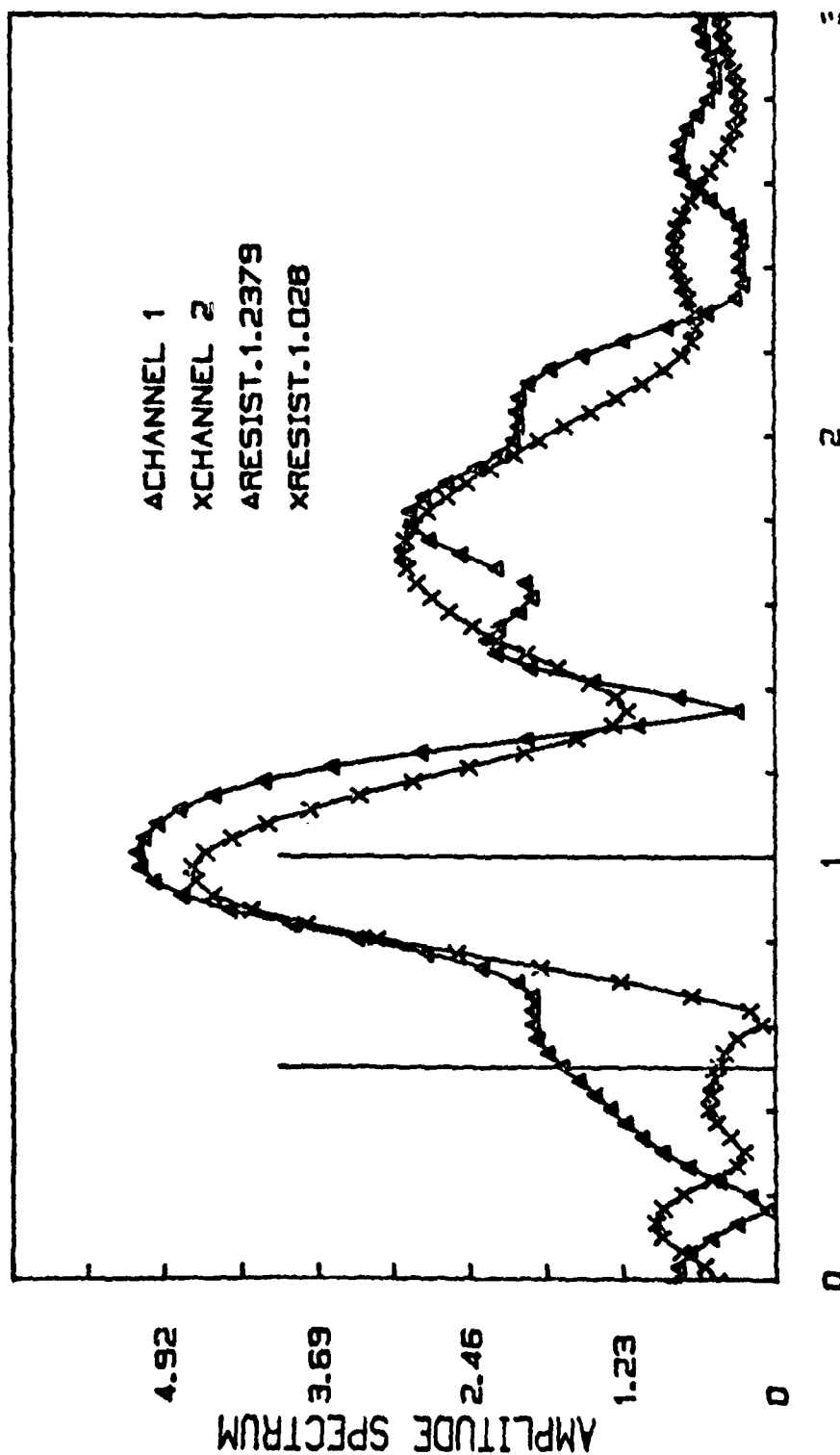
SPECTRUM AT FROUDE NR=0.376



S VALUE SERIES 60 CB60 RUN 14 $L = 10'$

Figure 5

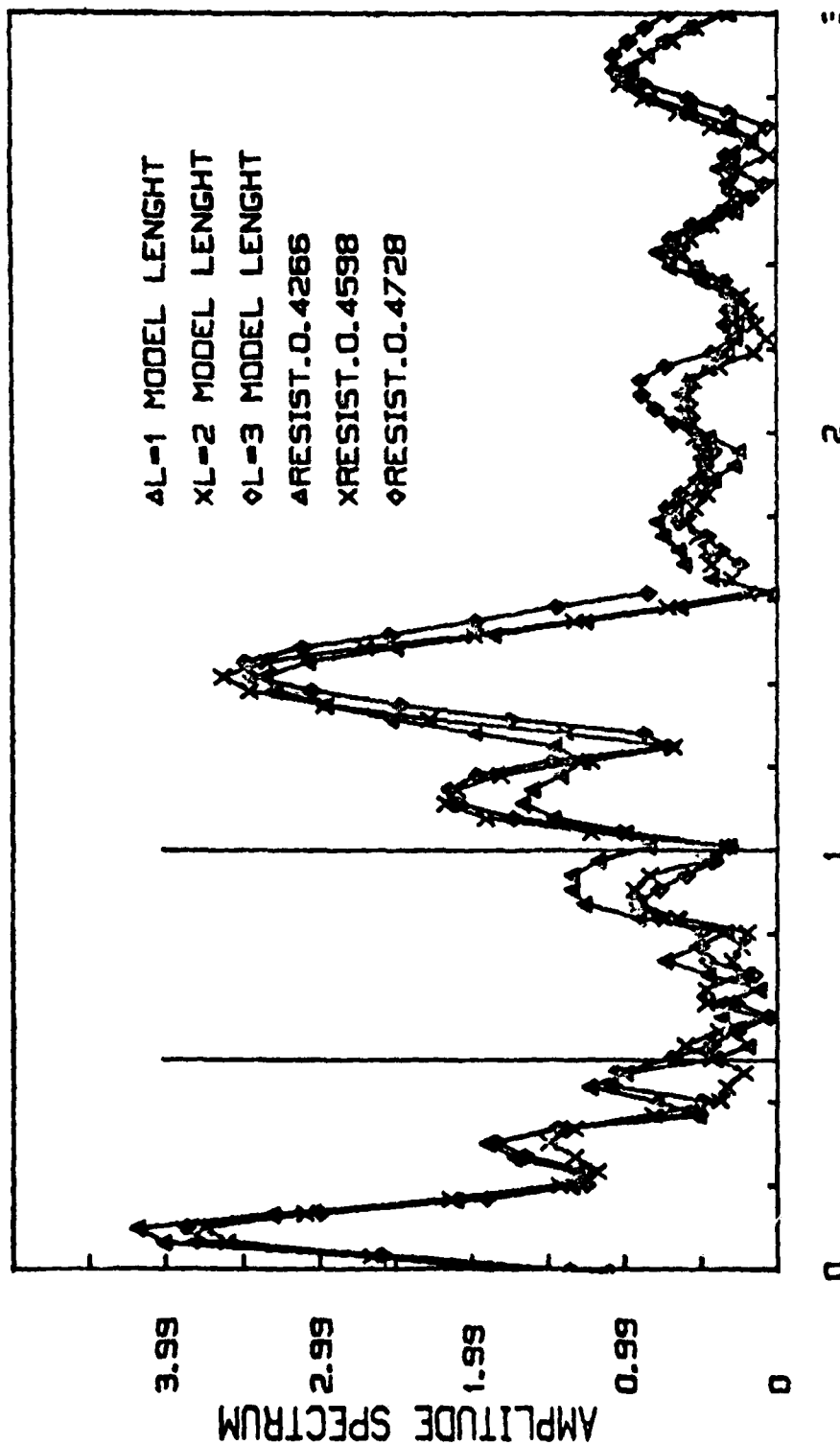
SPECTRUM AT FROUDE NR=0.377



S VALUE SERIES 60 CB60 RUN 15 L = 15'

Figure 6

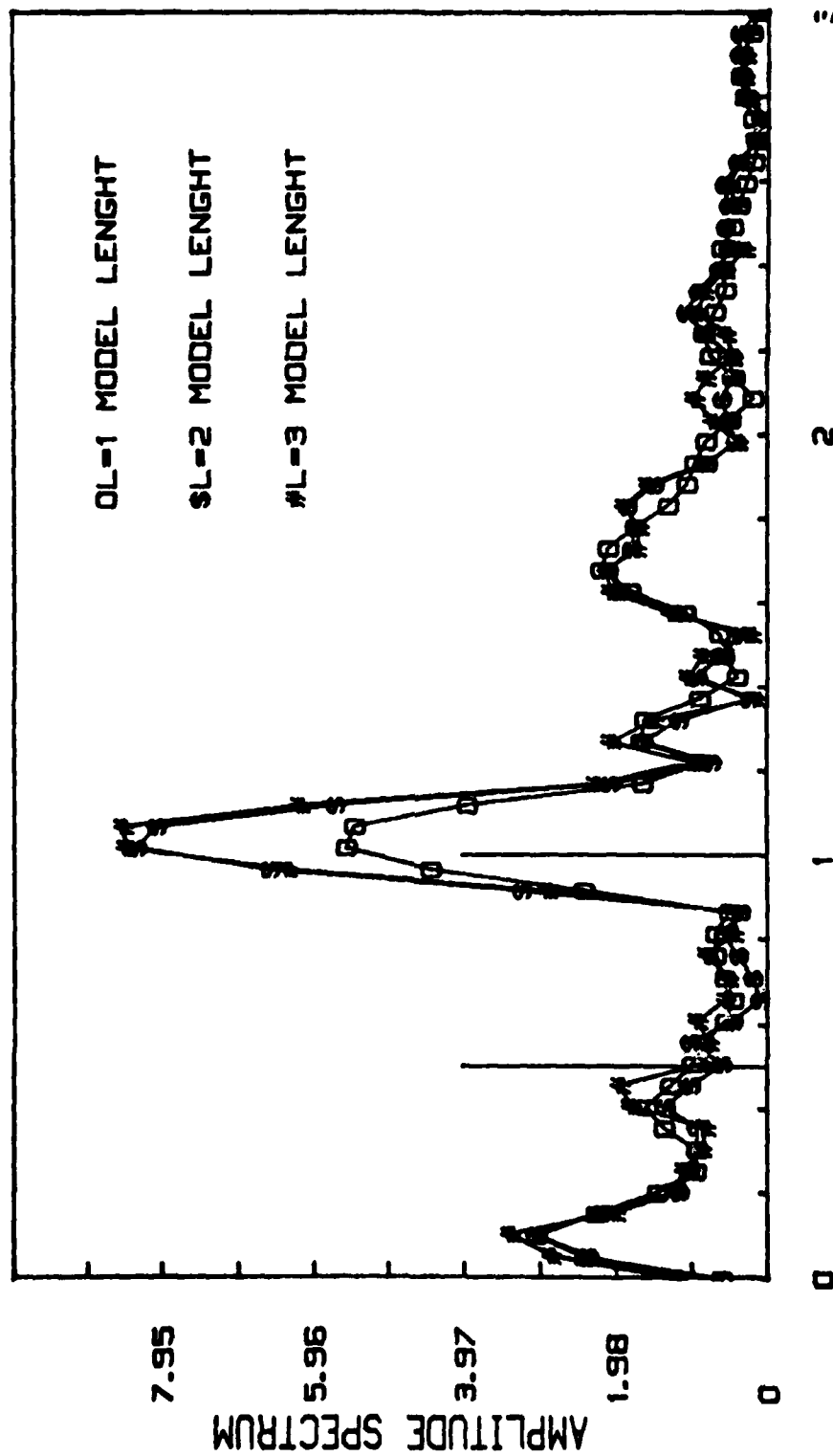
SPECTRUM AT FROUDE NR=0.245



S VALUE SERIES 60 CB60 RUN 1

Figure 7

SPECTRUM AT FROUDE NRO.272



S VALUE SERIES 60 CB60 RUN 4

Figure 8

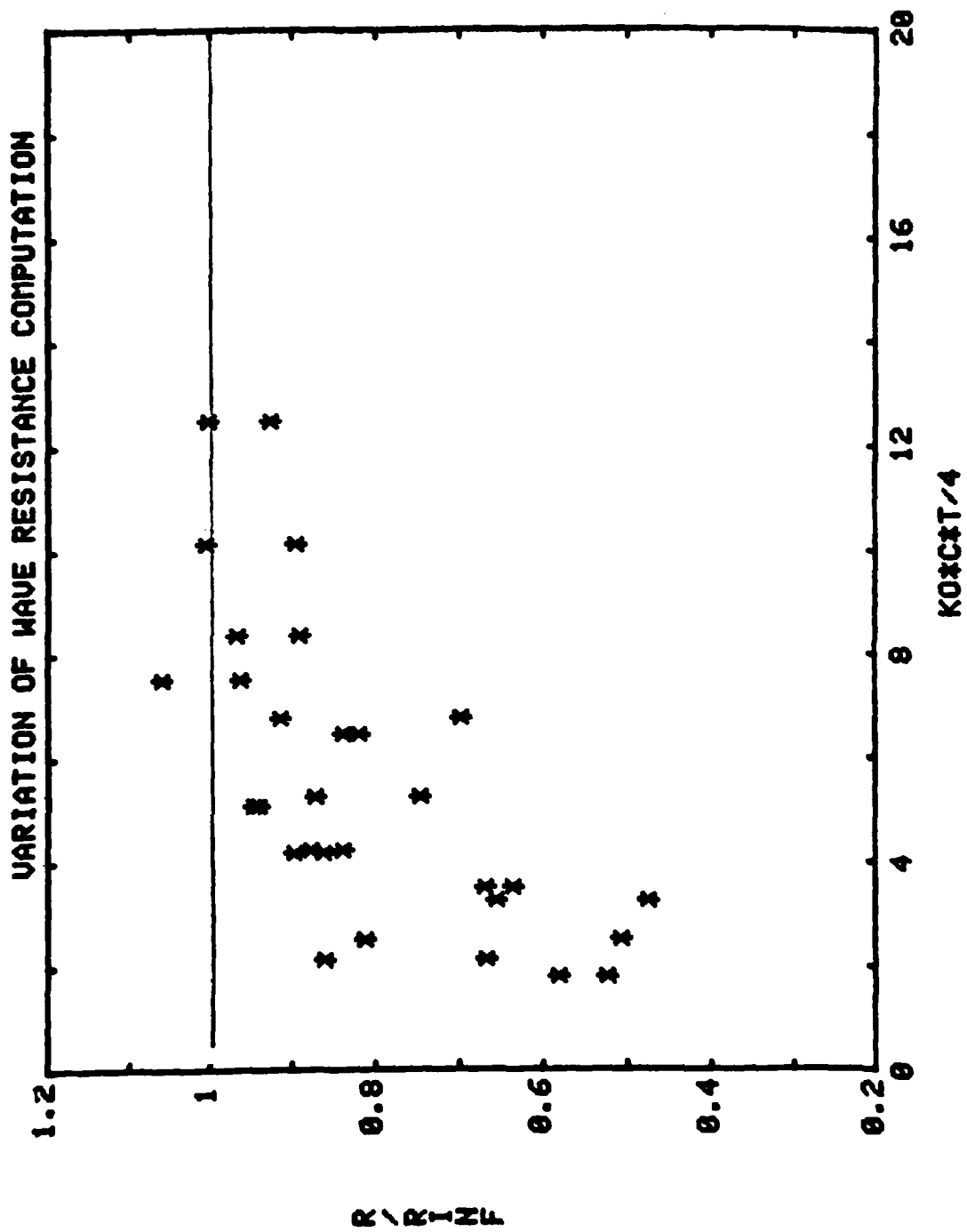


Figure 9

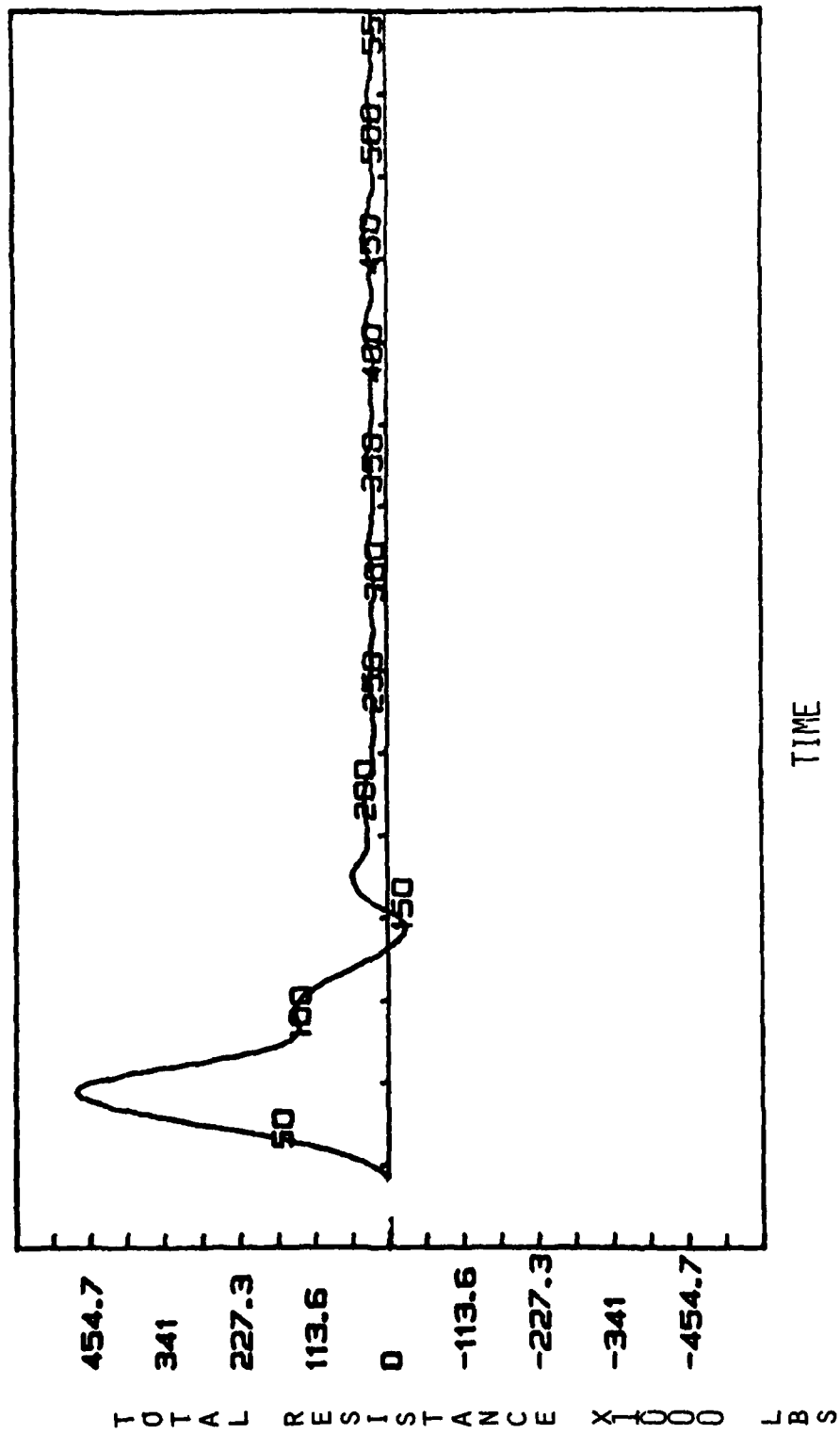


Figure 10

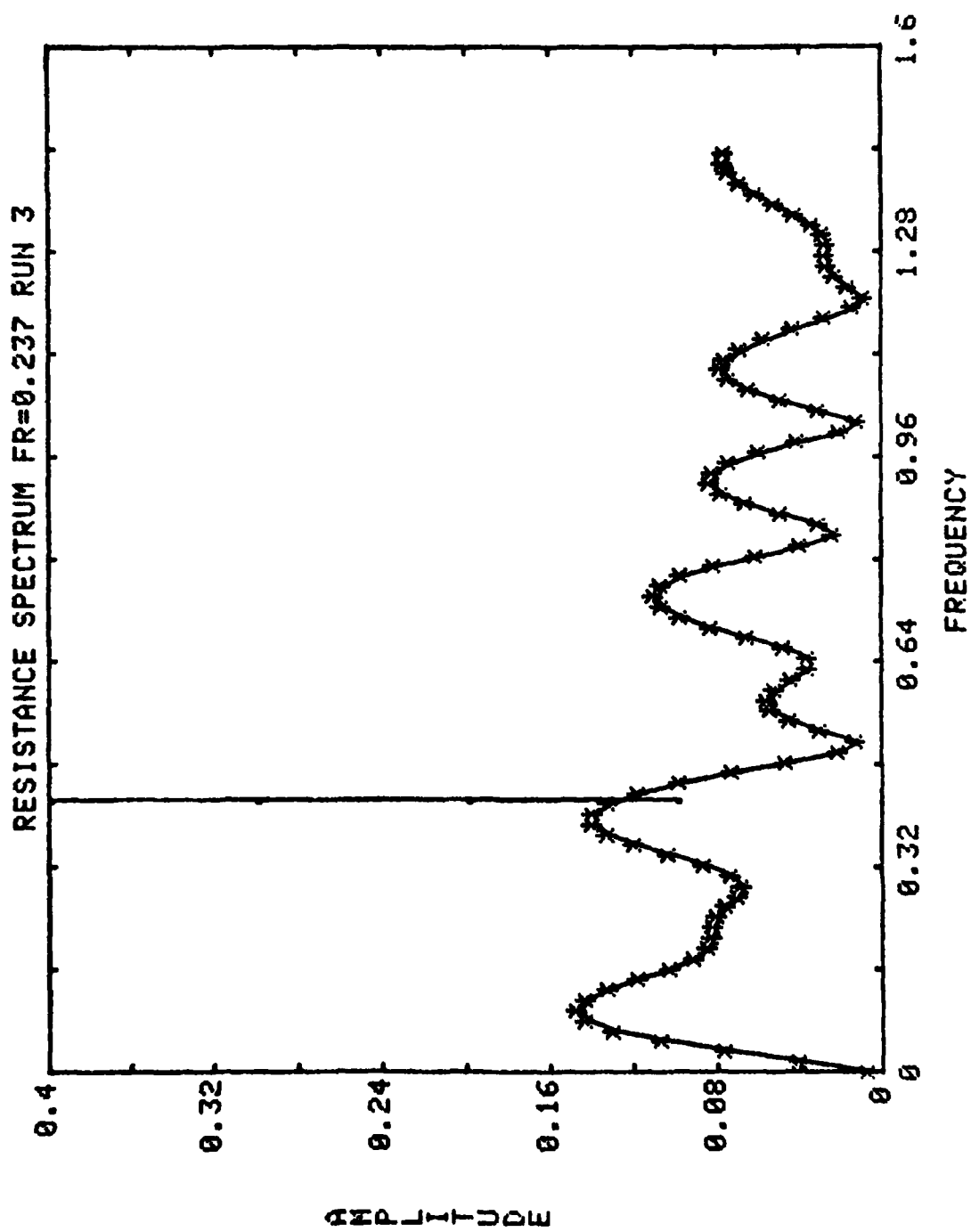


Figure 11

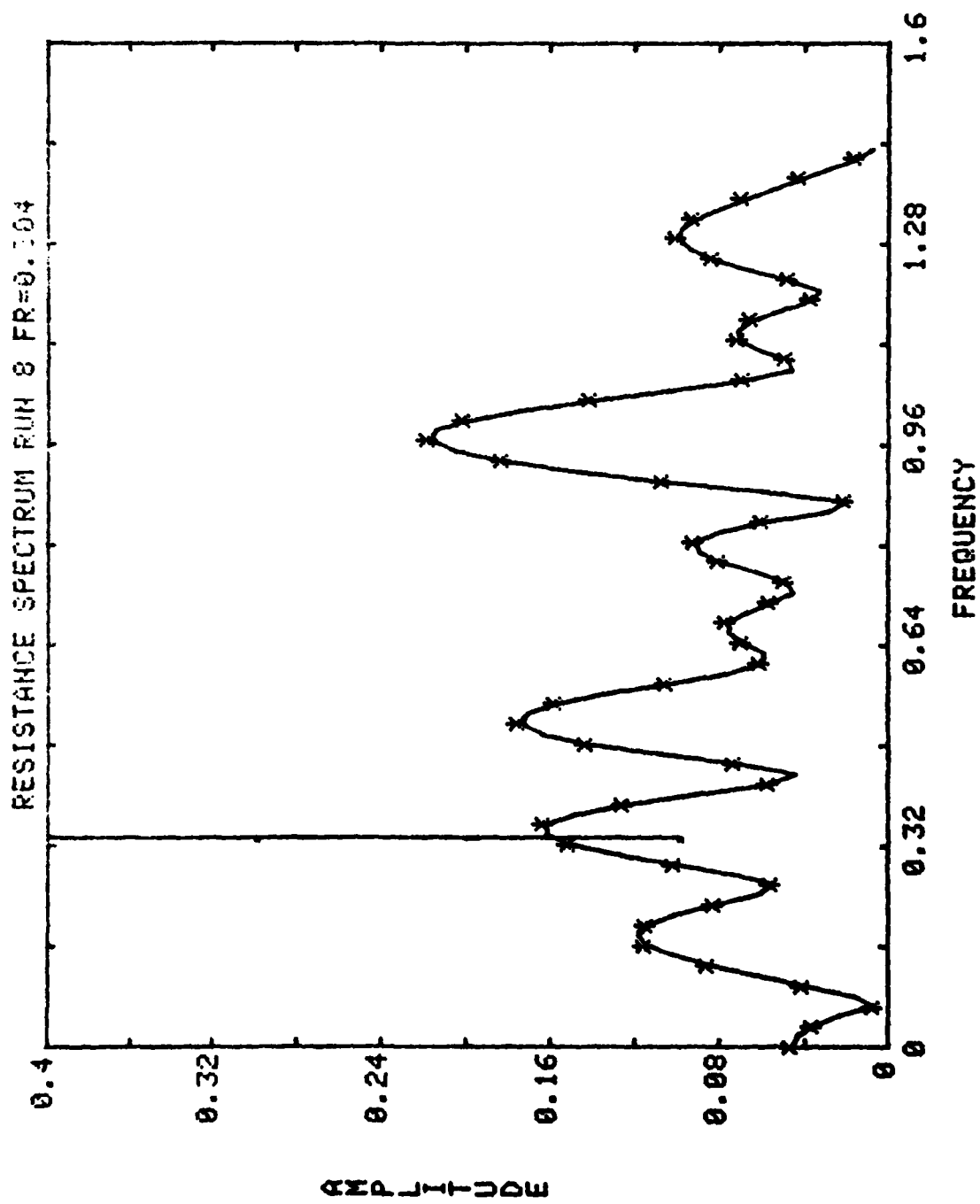


Figure 12

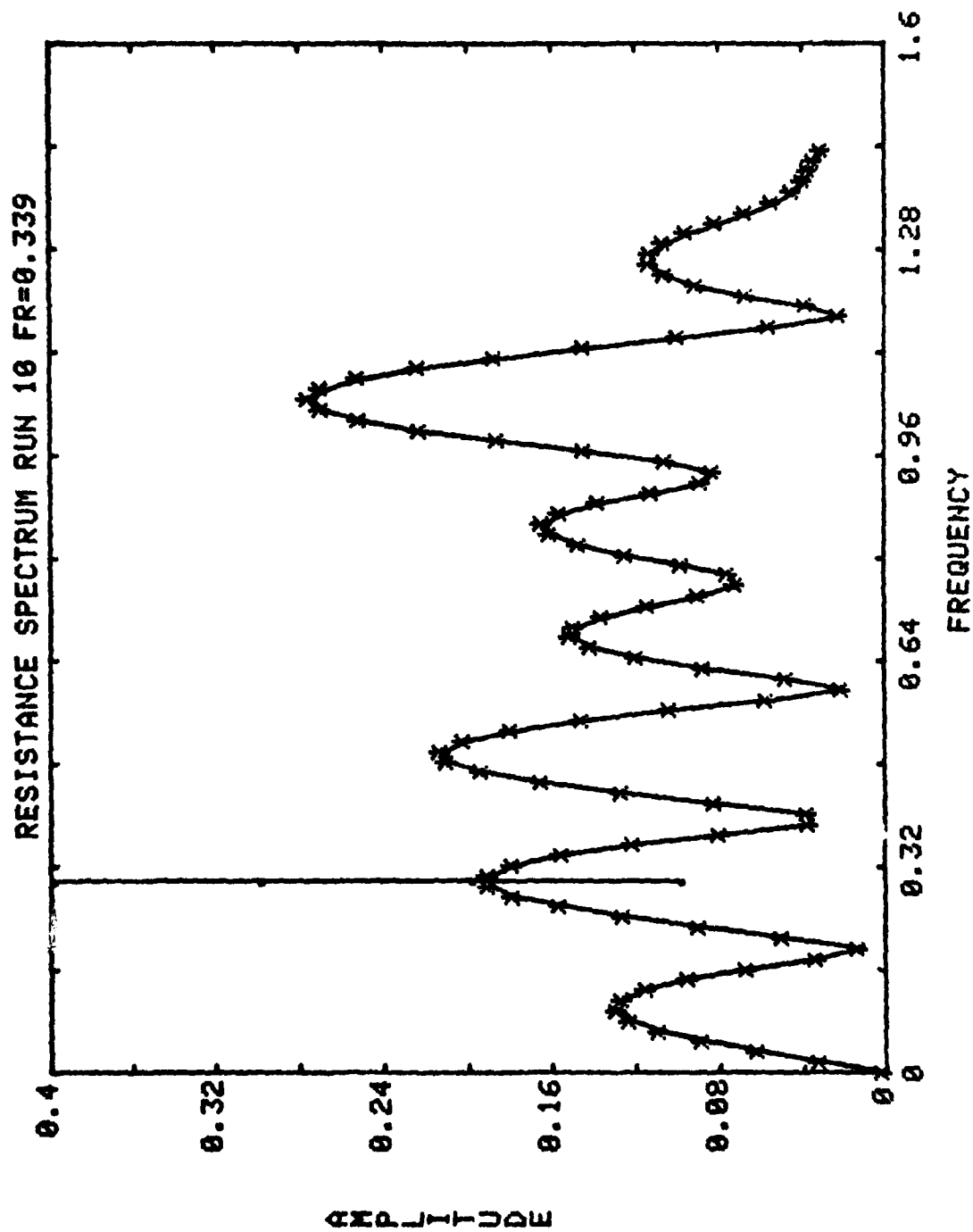


Figure 13

TEST:205 RUN NO: 4 DATE:23-DEC-78 TIME:10:53:05

◆ = DRAG.PSD ((LB2))-EVEN T205/S 0

▲ = MOMT.PSD ((FTLB2))-EVEN T205/S 0

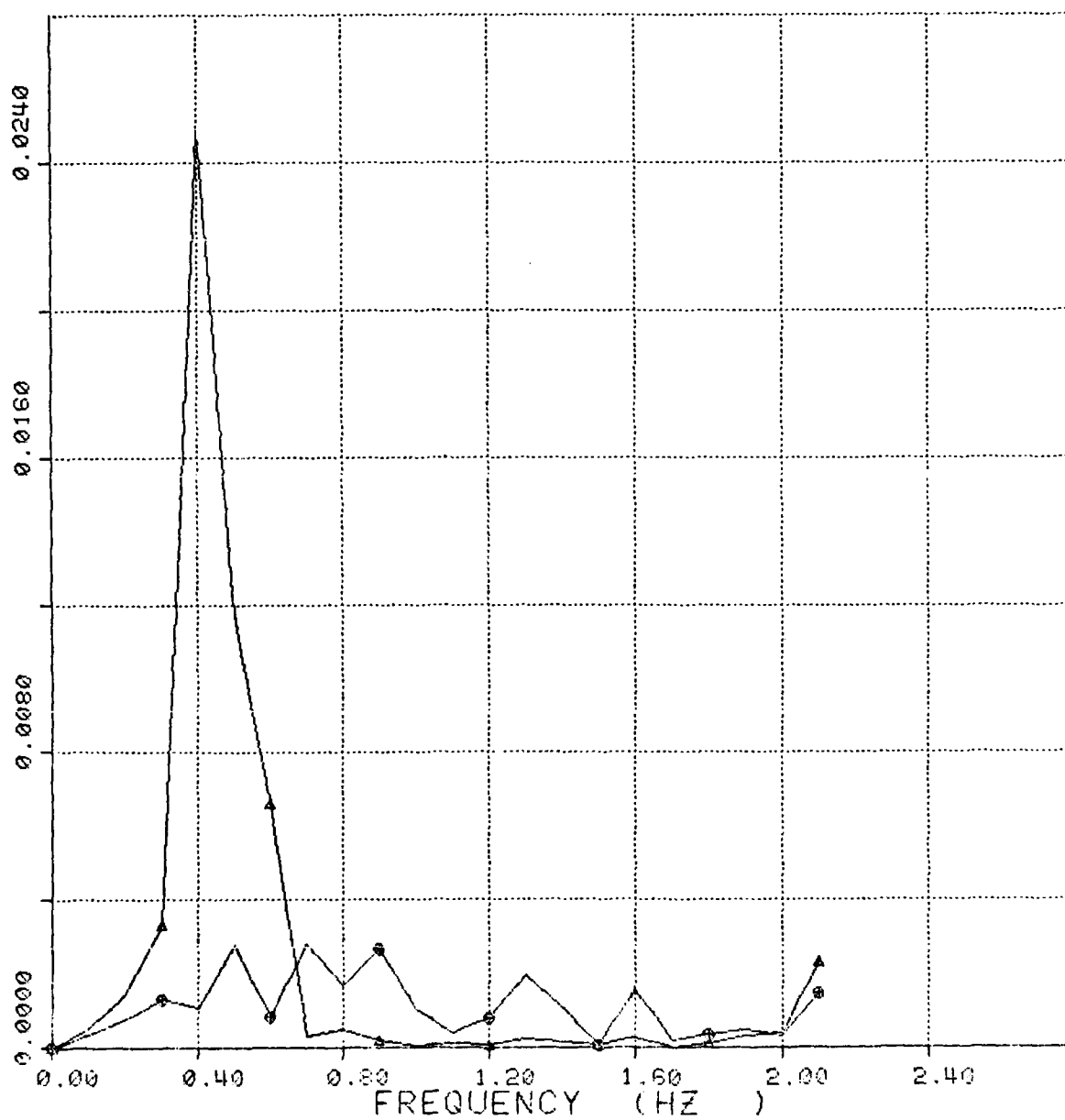


Figure 14
32

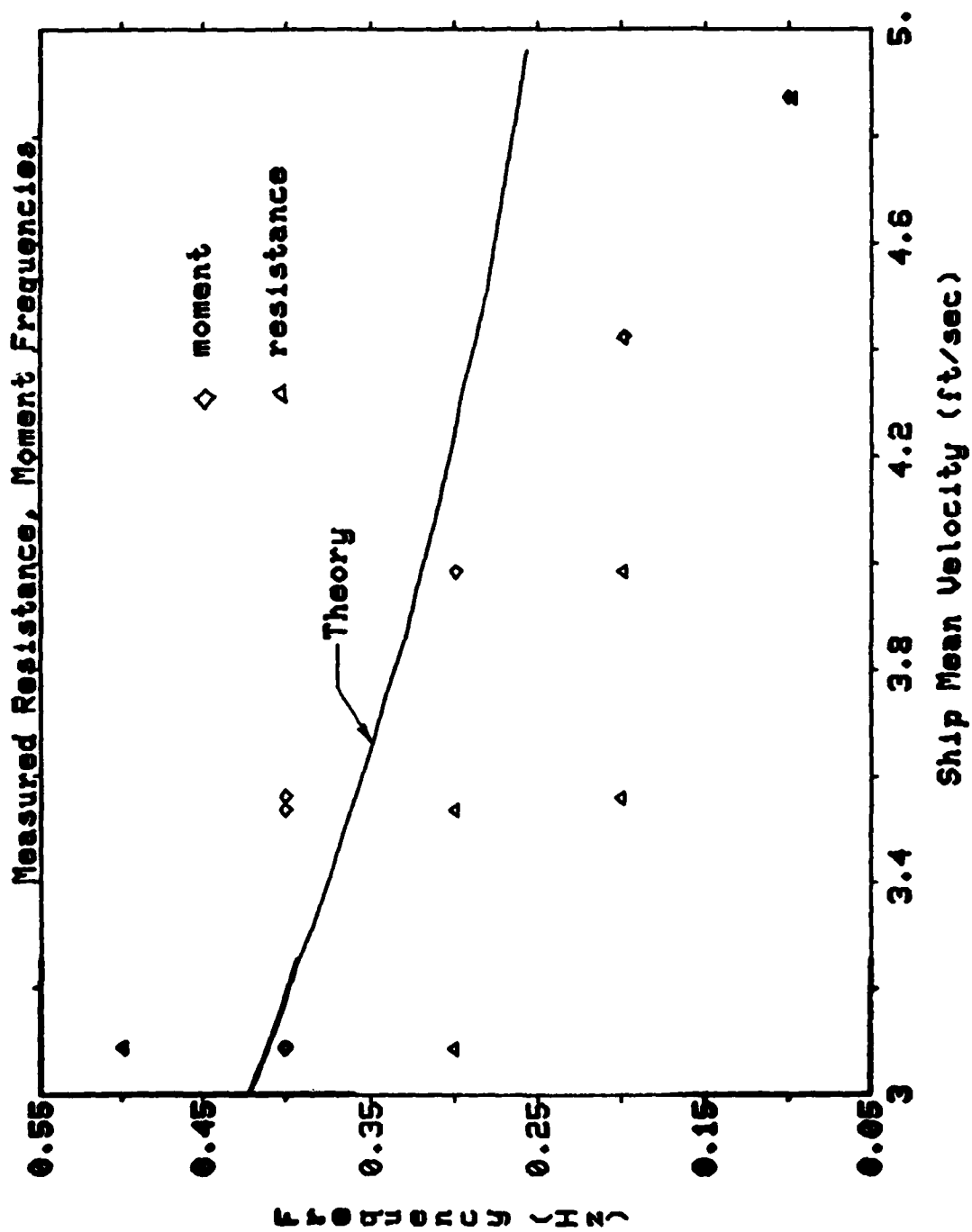


Figure 15



Figure 16
Isolated acceleration wave
34

TEST:213 RUN NO: 8 DATE:03-JAN-79 TIME:15:03:27

⊕ = WAV1.EU (FT)-ALL T213/S 0

△ = WAV2.EU (FT)-ALL T213/S 0

⊞ = WAV3.EU (FT)-ALL T213/S 0

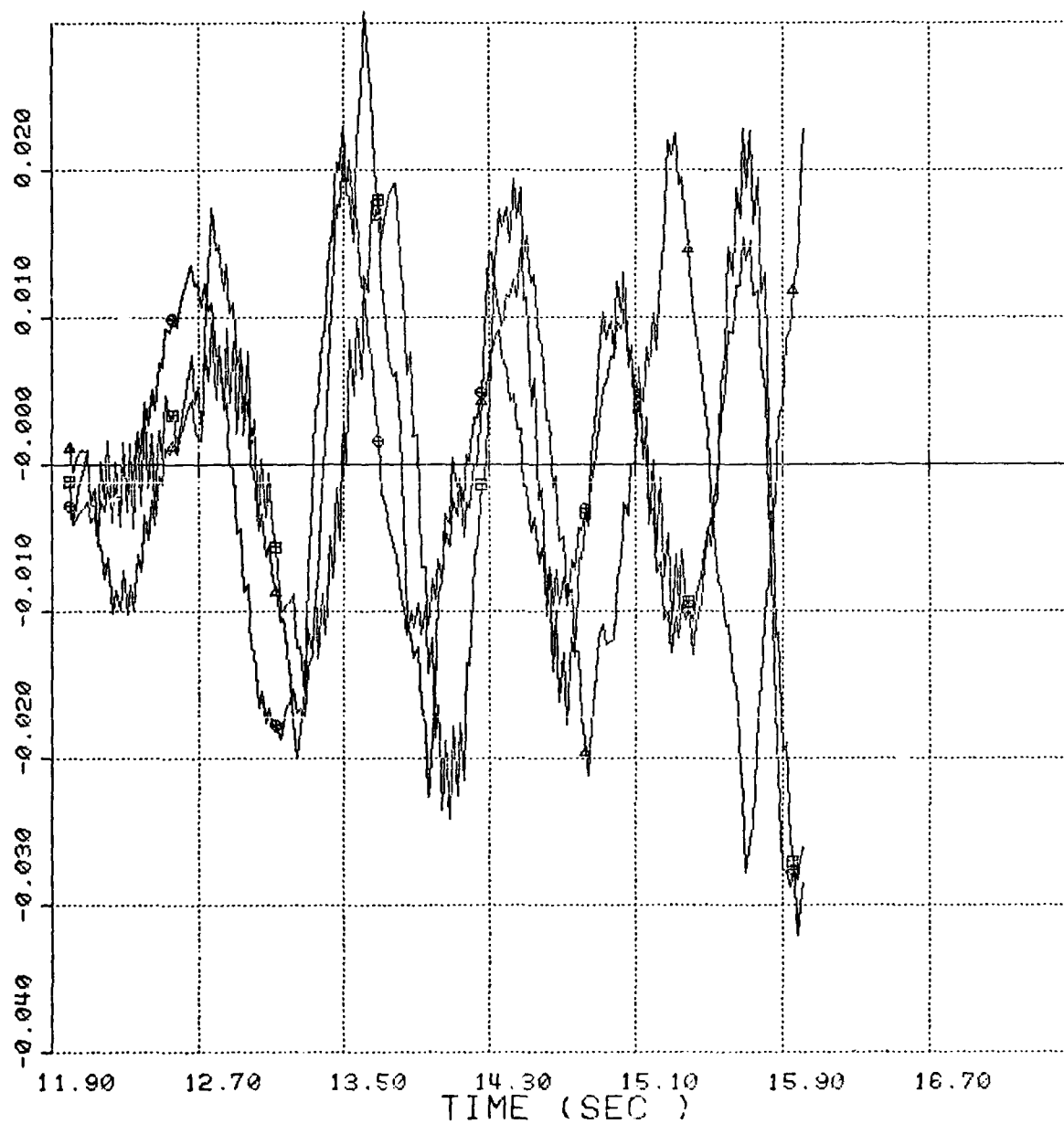


Figure 17

TEST:407 RUN NO: 0 DATE:24-APR-79 TIME:11:12:19

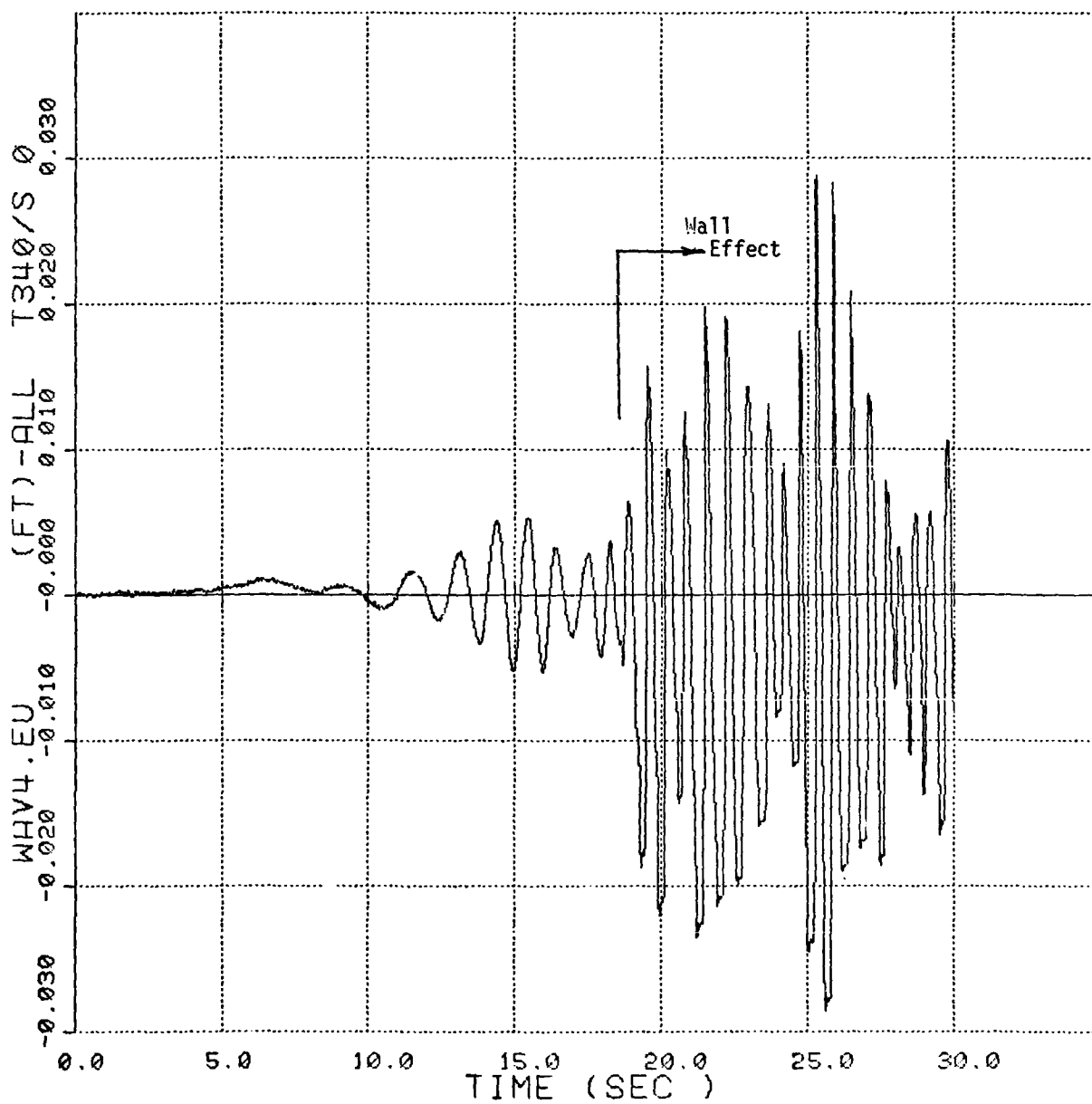


Figure 18

TEST:632 RUN NO: 0 DATE:04-OCT-79 TIME:16:01:12

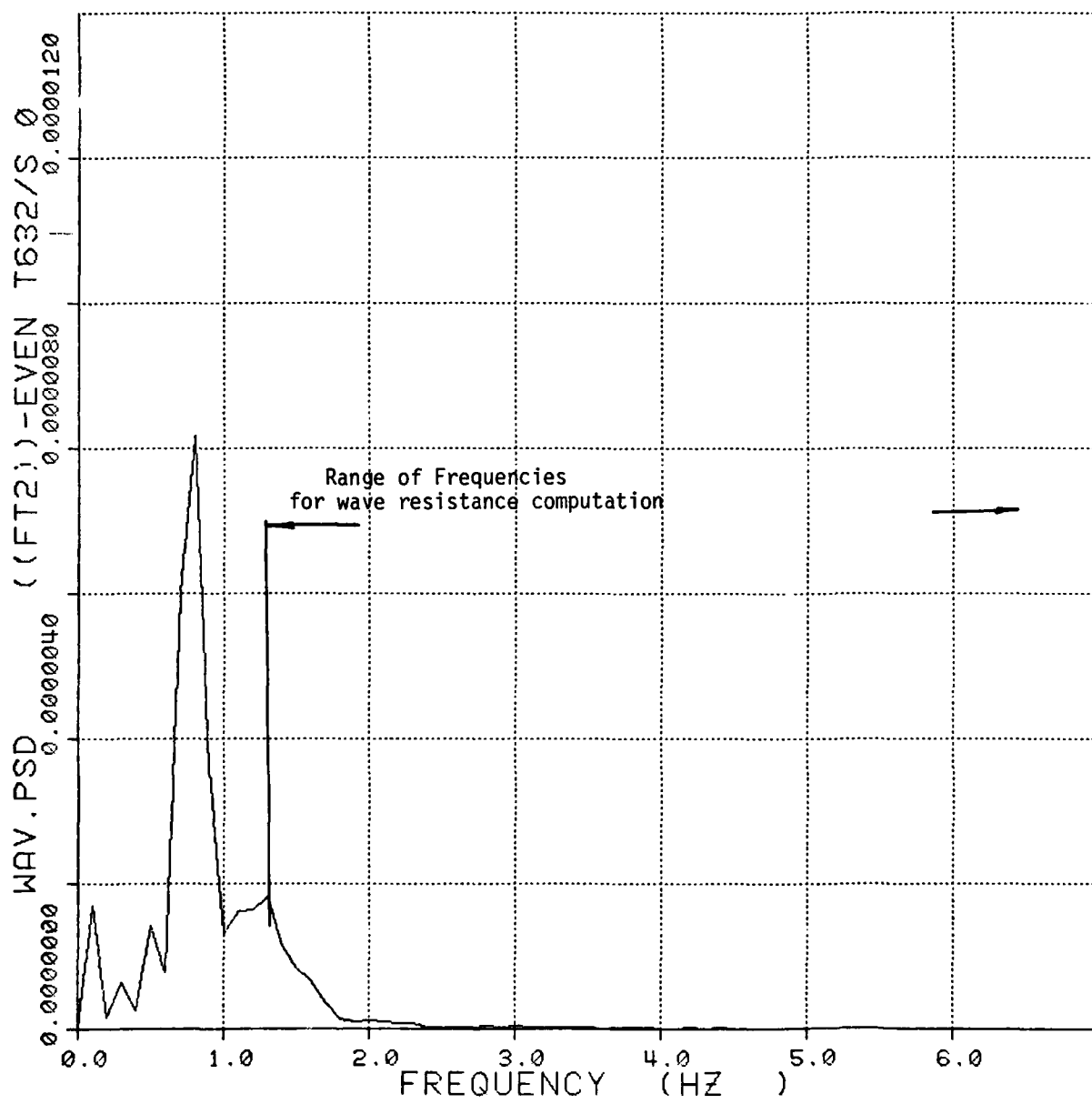


Figure 19

TEST:632 RUN NO: 0 DATE:04-OCT-79 TIME:16:05:34

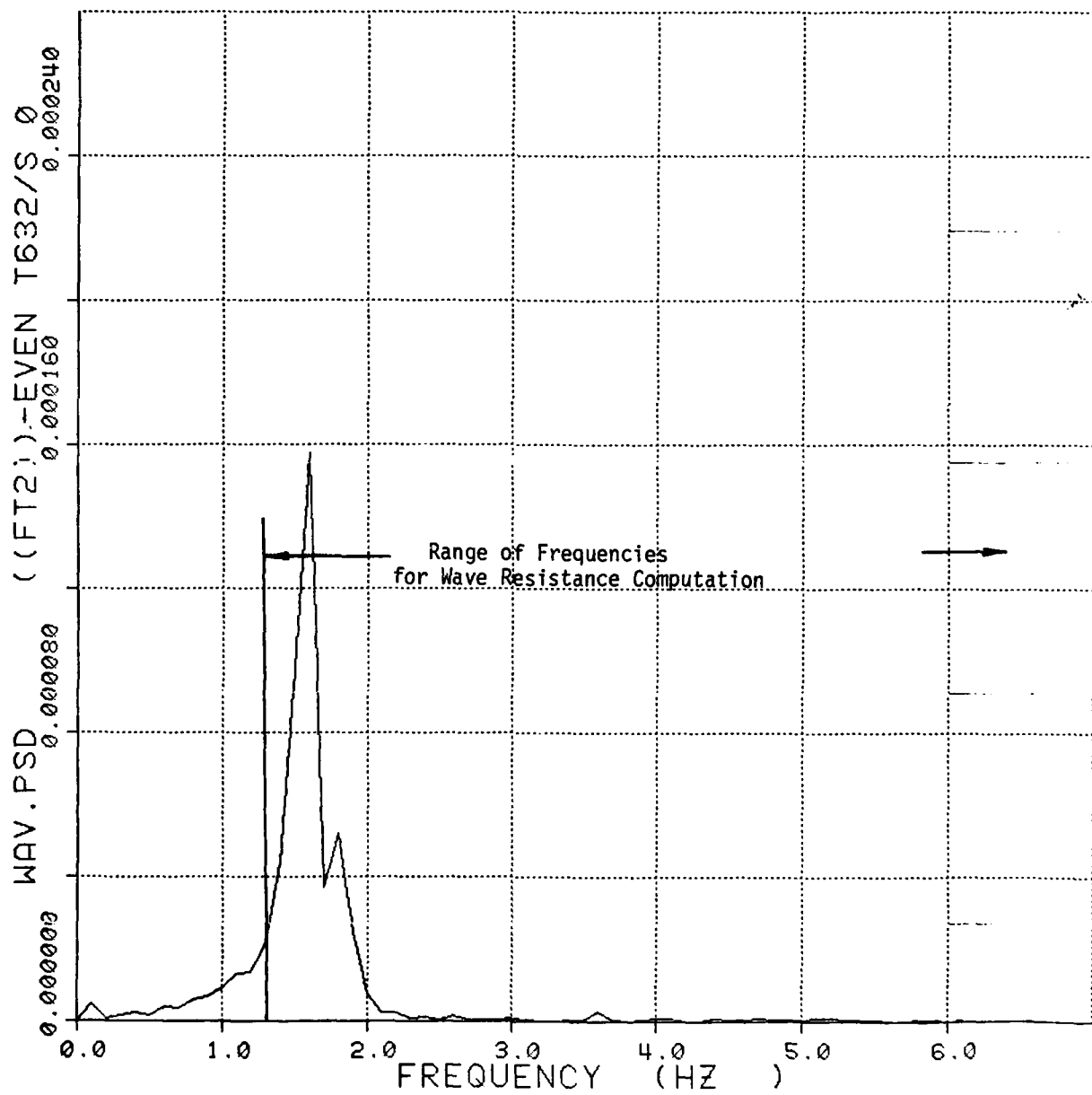


Figure 20

INITIAL DISTRIBUTION LIST

	<u>No. of Copies</u>
Defense Documentation Center Cameron Station Alexandria, Virginia 22314	20
Assistant Librarian Technical Processing Division U. S. Naval Academy Annapolis, Maryland 21302	4
Academic Dean U. S. Naval Academy Annapolis, Maryland 21402	1
Director of Research U. S. Naval Academy Annapolis, Maryland	1
Division Director Division of Engineering and Weapons U. S. Naval Academy Annapolis, Maryland 21402	1
Department Chairman Naval Systems Engineering Department U. S. Naval Academy Annapolis, Maryland 21402	2
Professor B. Adee University of Washington Mechanical Engineering Department Seattle, Washington 98195	1
Professor Ronald W. Yeung Ocean Engineering Department Massachusetts Institute of Technology Cambridge, Massachusetts 02139	1
Professor J. V. Wehausen University of California Naval Architecture Department Berkeley, California	1
Dr. June Bai Code 1552 Naval Ship Research and Development Center Bethesda, Maryland 20084	2

	No. of Copies
Dr. W. C. Lin Code 1524 Naval Ship Research and Development Center Bethesda, Maryland 20084	2
Professor T. Sabuncu Istanbul Teknik Universitesi Gemi Insaat Fakultesi Taksim Taksim Istanbul Turkey	2
Ove Sundstrom The Royal Institute of Technology in Stockholm Department of Hydromechanics S-10044 Stockholm 70, Sweden	1
K. W. Eggers Institut für Schiffbau der Universität Hamburg 2 Hamburg 60, Lammertsh 90 Germany	1